ACS APPLIED MATERIALS & INTERFACES

Research Article

www.acsami.org

Sulfur–Carbon Nanocomposite Cathodes Improved by an Amphiphilic Block Copolymer for High-Rate Lithium–Sulfur Batteries

Yongzhu Fu, Yu-Sheng Su, and Arumugam Manthiram*

Electrochemical Energy Laboratory & Materials Science and Engineering Program, The University of Texas at Austin, Austin, Texas 78712, United States

ABSTRACT: A sulfur–carbon nanocomposite consisting of a commercial high-surface-area carbon (i.e., Black Pearls 2000, BET surface area >1000 m^2 g^{-1}) and sulfur has been synthesized by an in situ deposition method. The nanocomposite is in the form of agglomerated nanoparticles, with the micropores within the carbon filled with sulfur and the mesopores on the carbon surface almost completely covered by sulfur. The BET surface area of the nanocomposite containing a sulfur content of 63.5 wt % is significantly reduced to only 40 m^2 g^{-1}. Cathodes containing the nanocomposite and Pluronic F-127 block copolymer, which partially replaces the polyvinylidene fluoride binder, were prepared and evaluated in lithium cells by cyclic voltammetry and galvanostatic cycling. The nanocomposite cathodes with the copolymer show improved electrochemical stability and cyclability. The Pluronic copolymer helps retain a uniform nanocomposite structure within the electrodes, improving the electrochemical contact, which was manifested by scanning electron microscopy and electrochemical impedance spectroscopy. The sulfur-Black Pearls nanocomposite with the Pluronic copolymer as an additive in the electrodes is promising for high-rate rechargeable lithium–sulfur batteries.

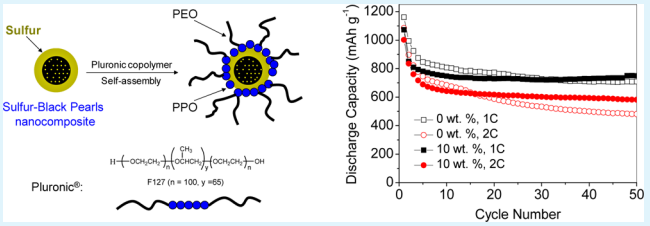

KEYWORDS: *rechargeable lithium–sulfur battery, nanocomposite, amphiphilic block copolymer, electrochemical performance, cyclability*

1. INTRODUCTION

Lithium-ion (Li-ion) batteries have revolutionized the portable electronics market for over 20 years because of their high energy density and good cycle life. Because of the foreseen shortage of oil resources and increasing concerns over environmental pollution, interests in electric vehicles and utilization of renewable energies like solar or wind are increasing. Going from portable batteries in cell phones or laptops to large-pack batteries in electric vehicles requires high energy density, good safety, and low cost. Li-ion batteries based on traditional insertion oxide cathode materials with limited capacities of 100–200 mA h g^{-1} cannot meet these requirements. In this regard, alternative cathode materials such as oxygen and sulfur with a leap in capacity and low operating voltages have attracted much attention in recent years.[1]

Lithium–sulfur (Li–S) batteries have been studied for almost 50 years since Herbet and Ulam first introduced the concept of elemental sulfur as a positive electrode material in 1962.[2] By accommodating two electrons per atom, sulfur provides an order of magnitude higher capacity (ca., 1675 mA h g^{-1}) than the insertion oxide cathodes, which can enable packed cells with two to three times higher energy densities than the state-of-the-art Li-ion batteries. However, rechargeable Li–S batteries are limited by the low utilization of sulfur and poor cycle life for large-scale applications.[3] In addition, the rate capability of Li–S batteries is constrained by the low electrical conductivity of sulfur and the discharged products. Unlike the insertion compound electrodes, sulfur undergoes a series of structural and morphological changes during the charge–discharge process, involving the formation of lithium polysulfides Li_2S_x (x = 8, 6, 4, and 3) and sulfides Li_2S_2/Li_2S, which are all insulators.[4] In addition, lithium polysulfides are soluble in liquid electrolyte whereas sulfur and sulfides are not. The dissolved high-order polysulfides (e.g., Li_2S_8 and Li_2S_6) could shuttle to the metallic lithium anode and get reduced to low-order polysulfides (e.g., Li_2S_4 and Li_2S_3), which could travel back to the cathode and get oxidized, resulting in infinite cycling.[5,6] To overcome these problems, we need advanced sulfur-based cathodes with high electrical conductivity and reduced polysulfide dissolution to move the Li–S technology close to mass commercialization.

An effective strategy for improving the sulfur electrodes is to prepare sulfur–carbon nanocomposites with intimate contact between sulfur and carbon and confinement structures for polysulfides.[7−13] For example, Ji et al.[7] developed a mesoporous carbon framework that constrains sulfur nanofiller growth within its channels, generating essential electrical contact between them and trapping polysulfides and thereby exhibiting reversible capacities up to 1320 mA h g^{-1}. Jayaprakash et al.[10]

Received: August 17, 2012
Accepted: October 23, 2012
Published: October 23, 2012

   dx.doi.org/10.1021/am301688h | *ACS Appl. Mater. Interfaces* 2012, 4, 6046–6052

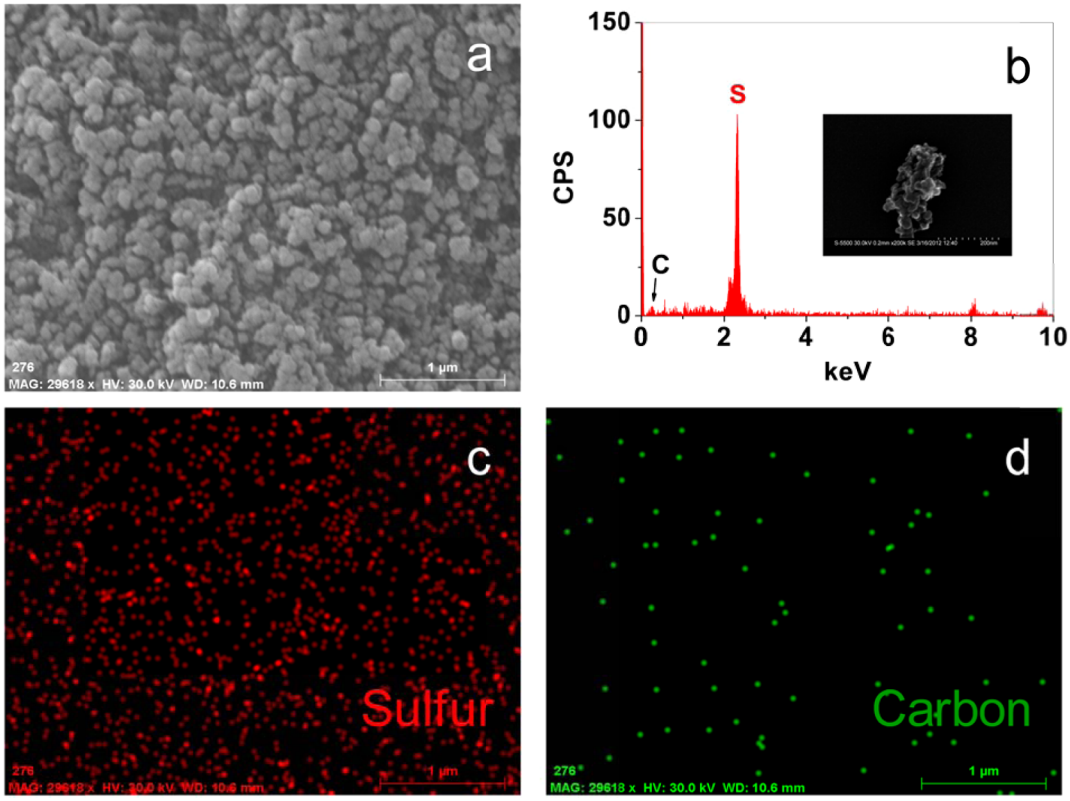

Figure 1. (a) SEM image, (b) EDX spectrum, (c) sulfur mapping, and (d) carbon mapping of the synthesized sulfur-Black Pearls (S-BP) nanocomposite; the inset in (b) shows a high-resolution SEM image of the agglomerated S-BP nanoparticles.

utilized mesoporous hollow carbon capsules that encapsulates and sequesters elemental sulfur in its interior and porous shell, exhibiting an initial discharge capacity of 1071 mA h g^{-1} and maintaining a reversible capacity of 974 mA h g^{-1} at a rate of *C*/2 over 100 cycles. Improvements in the trapping of polysulfides have also been achieved with sulfur−carbon nanocomposites by attaching poly(ethylene glycol) or ionic polymers (e.g., poly(3,4-ethylenedioxythiophene)-poly(styrene sulfonate)) to the surface of the composites.[7,14,15] The polymer modification of the carbon surface provides a chemical gradient that retards diffusion of the large polysulfide anions out of the electrode.

We report here a sulfur−carbon nanocomposite, utilizing a commercial high-surface-area Black Pearls 2000 carbon and prepared by an in situ deposition method in aqueous solution. Pluronic F-127 block copolymer, which partially replaces polyvinylidene fluoride (PVdF) binder, is used in the electrode preparation to improve the retention of polysulfides in the composite electrodes. The results demonstrate that Pluronic amphiphilic copolymers are beneficial to achieving high-rate electrochemical performance with Li−S batteries.

2. EXPERIMENTAL SECTION

2.1. Synthesis of Sulfur-Black Pearls Nanocomposite. Black Pearls 2000 carbon was obtained from Cabot Corporation. The sulfur−carbon nanocomposite with a calculated sulfur:carbon weight ratio of 7:3 was synthesized by a method similar to that reported previously.[16] In a typical reaction, sodium thiosulfate pentahydrate (4.963 g, 20 mmol) was dissolved in 800 mL of deionized water with magnetic stirring. Black Pearls (0.274 g) was dispersed in the reaction solution by sonication for 10 min. Four mL of concentrated hydrochloric acid was then added, and the reaction proceeded at room temperature overnight. The product formed was filtered, rinsed thoroughly with deionized water/ethanol/acetone, and dried in an air oven at 50 °C for 24 h. Pristine sulfur was synthesized by the same method without carbon for a comparison.

2.2. Characterization Techniques. Morphological characterizations were carried out with a FEI Quanta 650 scanning electron microscope (SEM) with energy-dispersive X-ray (EDX) spectroscopy and a Hitachi S-5500 SEM. The surface area and pore diameter were analyzed by a surface area analyzer (NOVA 2000, Quantachrome) using physical adsorption/desorption of N_2 at the liquid-N_2 temperature. The specific surface area and pore size distribution were calculated according to, respectively, the Brunauer−Emmett−Teller (BET) method and Barrett−Joyner−Halenda (BJH) method. The X-ray diffraction (XRD) data were collected between 20 and 70° at a scan rate of 0.04° s^{-1} on a Philips X-ray diffractometer equipped with CuKα radiation. The thermogravimetric analysis (TGA) data were collected with a Perkin-Elmer TGA 7 Thermogravimetric Analyzer at a heating rate of 5 °C min^{-1} from 30 to 600 °C with an air flow of 20 mL min^{-1}.

2.3. Electrode Fabrication and Characterizations of Electrochemical Properties. The plain sulfur−carbon cathodes were prepared by mixing the synthesized composite (60 wt %), Super P carbon (20 wt %), and PVdF binder (20 wt %). The mixture was dispersed in N-methylpyrrolidone (NMP) overnight to prepare slurry, which was then coated onto an aluminum foil followed by evaporating the NMP at 50 °C in an air oven for 24 h. The electrodes containing 5, 10, and 15 wt % of Pluronic F-127 (BASF) block copolymers were prepared by a similar process, but by replacing the PVdF binder by the same amount of Pluronic F-127 in the slurry. The electrodes were pressed and cut into circular disks with a diameter of 12 mm. CR2032 coin cells were assembled with the cathodes, lithium foil anode, 1.0 M lithium trifluoromethanesulfonate and 0.1 M lithium nitrate in dimethoxy ethane and 1,3-dioxolane (1:1 v/v) electrolyte, and Celgard polypropylene separator. Cyclic voltammetry data were collected on a VoltaLab PGZ 402 potentiostat between 1.5 and 3.0 V at a scanning rate of 0.2 mV s^{-1}. Electrochemical performances of the cells were evaluated between 1.5 and 2.8 V at various C rates (C = 1675 mA g^{-1}).

dx.doi.org/10.1021/am301688h | *ACS Appl. Mater. Interfaces* 2012, 4, 6046−6052

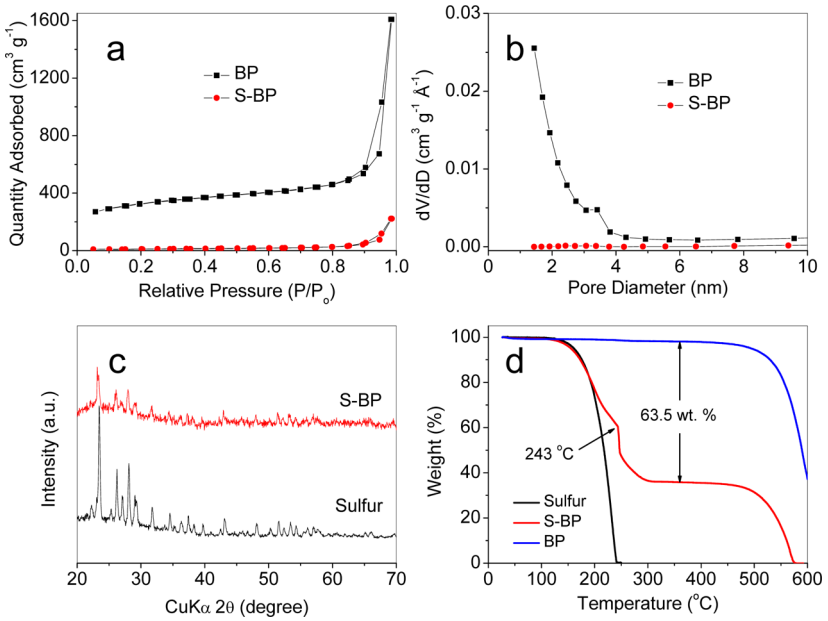

Figure 2. (a) N_2 adsorption/desorption isotherm and (b) pore size distribution of the BP and S-BP nanocomposite, (c) XRD patterns, and (d) TGA of pristine sulfur, S-BP nanocomposite, and BP.

Electrochemical impedance spectroscopy (EIS) data were collected with a computer interfaced HP 4192A LF Impedance Analyzer in the frequency range of 1 MHz to 0.1 Hz with an applied voltage of 5 mV and lithium foil as both counter and reference electrodes.

3. RESULTS AND DISCUSSION

Black Pearls is a high-surface-area (>1000 m^2 g^{-1}), nanosized (~30 nm diameter) carbon, which has been widely used as an additive in gas diffusion layer and catalyst support in fuel cells[17−19] and as electrode materials in electrochemical double layer capacitors.[20] Its microporous structure is ideal for incorporating elemental sulfur to render a sulfur-Black Pearls (S-BP) nanocomposite. Accordingly, the S-BP nanocomposite with a calculated S:BP weight ratio of 7:3 was synthesized by an in situ deposition of sulfur involving the reduction of sodium thiosulfate ($Na_2S_2O_3$) in aqueous solution.[16]

Figure 1a shows the SEM image of the S-BP composite synthesized. The composite is in the form of agglomerated nanparticles with a particle size of a few hundred nanometers. Unlike the sulfur-Super P composite synthesized by the same method,[16] no microsized pure sulfur particles wrapped by carbon were formed within the S-BP composite, indicating that the BP facilitates the nucleation of sulfur within Black Pearls nanoparticles during the in situ sulfur deposition and prevents the formation of large sulfur particles. The EDX spectrum of the composite sample in Figure 1b shows a large peak for elemental sulfur along with a minor peak for carbon, indicating that the surface of the composite is almost fully covered by pure sulfur. The high resolution SEM image in the inset reveals the fine features of a "single" agglomerated particle consisting of numerous nanoparticles of 20−40 nm diameter, which is in agreement with the reported particle size of Black Pearls.[17] The elemental mapping of sulfur and carbon in Figure 1c, d again reveal the rich sulfur and poor carbon on the surface of the sample.

Figure 2a shows the nitrogen adsorption isotherm for the Black Pearls and the S-BP composite. Black Pearls presents mixed type I and type II isotherms, respectively, for low and high relative pressure (P/P_0).[20] The majority volume is adsorbed at low P/P_0, indicating the extended microporous structure of Black Pearls. In the intermediate P/P_0 range, the sloped plateau is due to the contribution from the outer mesoporous surface. In contrast, the composite exhibits almost no absorption for the low and intermediate P/P_0 ranges, indicating no micropores and mesopores are present in the sample. A small hysteresis between the adsorption and desorption branches of the isotherm near the maximum relative pressure is seen for Black Pearls, depicting another mesoporous like behavior, but not for the composite. The BET surface area of the composite is only 40 m^2 g^{-1}, a significant decrease compared to that of Black Pearls (1114 m^2 g^{-1}). Figure 2b shows the pore size distribution of the Black Pearls and the S-BP composite. Black Pearls contains mostly micropores (<2 nm) with a significant amount of mesopores (between 2 and 4 nm). In contrast, the composite exhibits a flat pore-size distribution with no pore accumulation. These results confirm the micropores within the Black Pearls carbon are filled with sulfur and the mesopores on the carbon surface are covered by sulfur.

Figure 2c presents the XRD patterns of the pristine sulfur and the S-BP composite. The broad peak located at 24.4° is attributed to the graphite (002) reflection of Black Pearls.[19] The other reflections in the composite match with those of the *Fddd* orthorhombic pristine sulfur,[21] but with low peak intensity, indicating small sulfur crystallites within the composite. Figure 2d shows the TGA plots of pristine sulfur, S-BP composite, and Black Pearls. The first weight loss from the composite begins to occur at the melting point (i.e., 115 °C) of sulfur, which corresponds to the loss of sulfur from the composite surface. With increasing temperature, sulfur is lost from the mesopores as indicated by a sloping weight loss profile. A sharp second weigh loss occurs at 243 °C due to the loss of sulfur from the micropores. In contrast, Black Pearl does not show any significant weight loss up to 400 °C. The TGA features of the composite are another indication of the microstructure of Black Pearls and the accommodation of

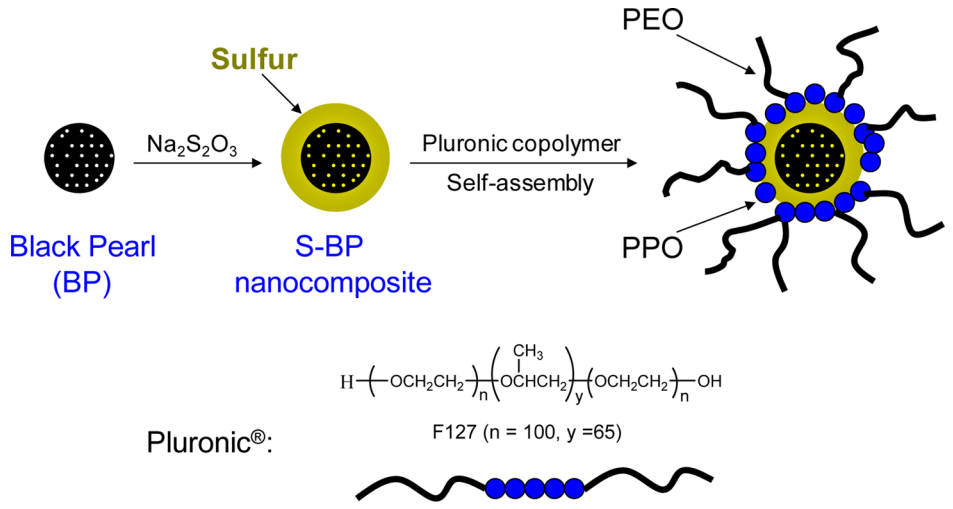

Figure 3. Schematic illustration of the synthesis of the S-BP composite and self-assembly of Pluronic F127 block copolymer on the surface of the S-BP nanoparticles.

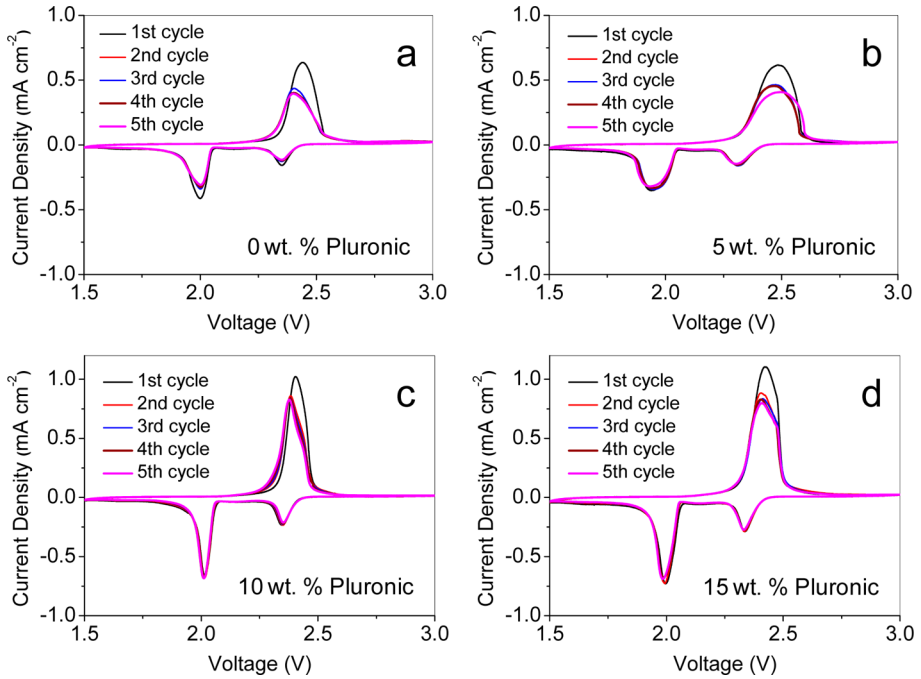

Figure 4. First five cycles of the cyclic voltammograms at a sweep rate of 0.2 mV s^{-1} of (a) the S-BP electrode without the Pluronic copolymer, and (b–d) the S-BP composite electrodes with various amounts of the Pluronic copolymer; the percentages indicated refer to Pluronic copolymer content.

sulfur within its micropores. The flat plateau above 300 °C shows the complete removal of sulfur from the composite, which represents a sulfur content is 63.5 wt % in the composite. The relatively low weight percent of sulfur within the composite indicates the volume of the inner micropores is not large enough to accommodate high weight percent (>70 wt %) of sulfur.

Sulfur on the surface of the S-BP composite is amenable to form lithium polysulfides during discharge, which could dissolve in the liquid electrolyte. Pluronic F-127, an amphiphilic block copolymer consisting of a hydrophobic poly(propylene oxide) (PPO) middle block and two hydrophilic poly(ethylene oxide) (PEO) end blocks, was used in the composite electrodes to reduce the dissolution of polysulfides. Pluronic copolymers are widely used as a template for synthesizing nanoparticles and to form micelles for drug delivery.[22,23] A thin film can be formed on the surface of hydrophobic particles (e.g., metal nanoparticles) by the hydrophobic association through the PPO block of the Pluronic copolymer.[24] Figure 3 depicts a schematic, showing the ideal self-assembly of the copolymer around the S-BP nanocomposites in the slurry preparation process. The S-BP nanocomposite is formed during the reduction of $Na_2S_2O_3$ in the in situ deposition process. Sulfur is embedded in the micropores and covered on the surface of the Black Pearls carbon. In electrodes, the hydrophobic PPO block of the copolymer adheres to the hydrophobic sulfur surface of the S-BP composite, whereas the hydrophilic PEO component could provide a chemical gradient that retards the diffusion of large polysulfide anions out of electrodes.[7] Polysulfides, which are ionic compounds and are partially

dx.doi.org/10.1021/am301688h | ACS Appl. Mater. Interfaces 2012, 4, 6046–6052

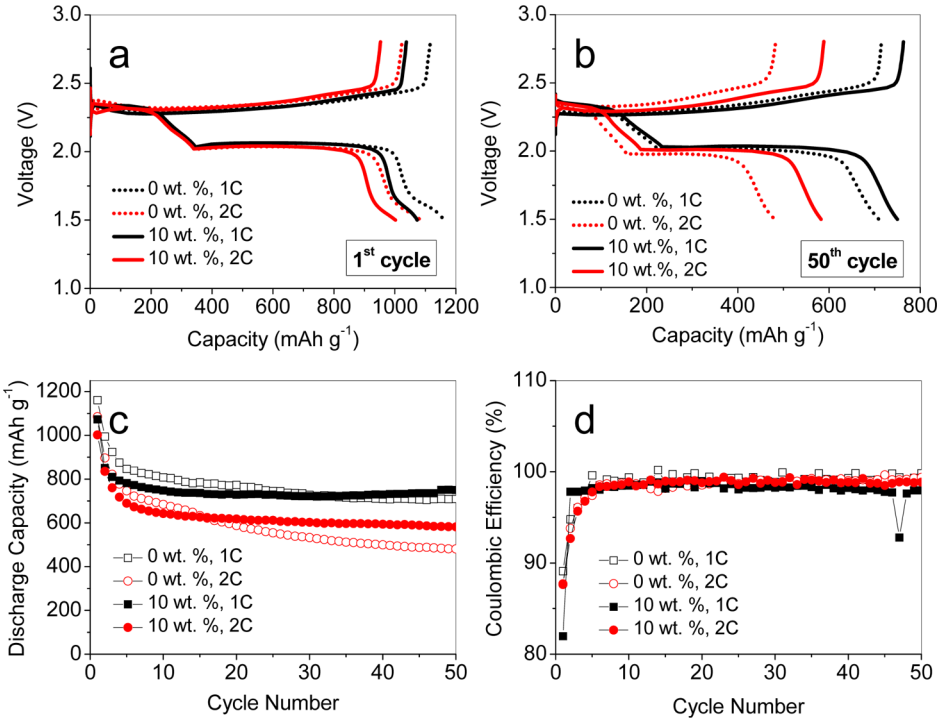

Figure 5. Voltage vs specific capacity profiles at 1*C* and 2*C* rates at (a) 1st cycle and (b) 50th cycle, (c) cyclability, and (d) Coulombic efficiencies of the S-BP composite electrodes with and without 10 wt % of Pluronic copolymer; the capacity values are in terms of the sulfur active mass.

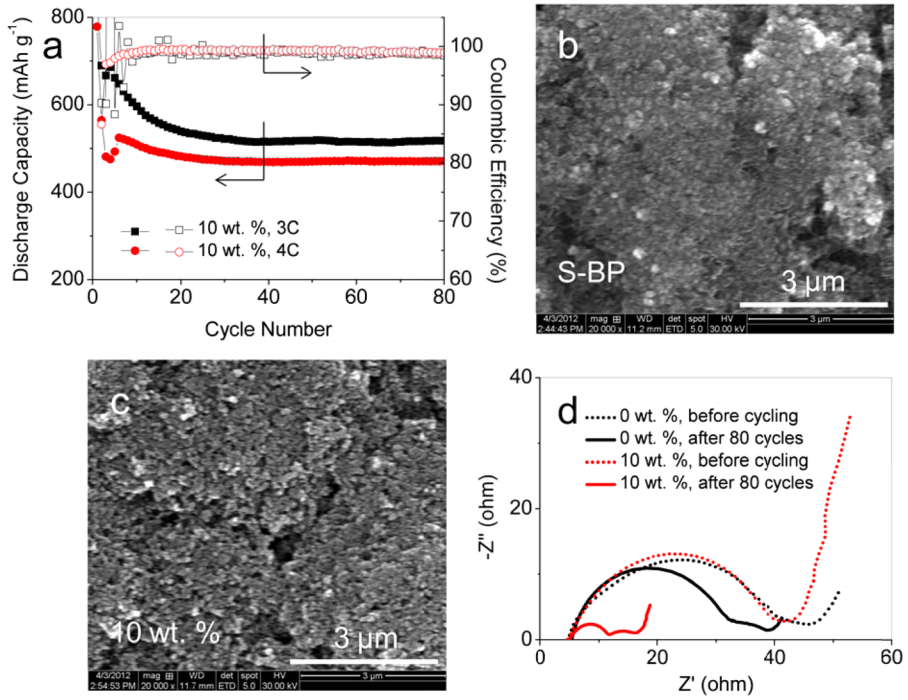

Figure 6. (a) Cyclability and Coulombic efficiencies of the S-BP composite electrodes with and without 10 wt % of Pluronic copolymer (the capacity values are in terms of the sulfur active mass), (b) SEM image of the S-BP electrode without Pluronic copolymer after 80 cycles, (c) SEM image of the S-BP electrode with 10 wt % Pluronic copolymer after 80 cycles, and (d) EIS analysis of the S-BP composite electrodes with and without 10 wt % Pluronic copolymer before and after 80 cycles.

hydrophilic, could form a gel-like mixture with the PEO component in presence of the liquid electrolyte. Such a gel should have much higher viscosity than the bulk electrolyte, which could reduce the migration of polysulfides. In addition, PEO is a good polymer electrolyte, which could improve the transport of lithium ions to the active material via the electrostatic coordination of lithium ions with ether oxygen atoms.[25]

Figure 4 shows the cyclic voltammograms (CV) of the S-BP and composite electrodes with and without 5, 10, and 15 wt % Pluronic copolymers for first five cycles. The voltage was first swept down to 1.5 V from the open circuit voltages, which are

dx.doi.org/10.1021/am301688h | ACS Appl. Mater. Interfaces 2012, 4, 6046−6052

not shown. In the subsequent anodic sweep, broad oxidation peaks are observed for the S-BP composite electrode without Pluronic copolymer and 5 wt % Pluronic copolymer. In contrast, rather narrow peaks with a shoulder are seen for the composite electrodes with 10 and 15 wt % copolymers, implying overlapped dual anodic peaks, which have been observed with other sulfur composites, especially those with confined structures.[10,26] All cycles show two regular reduction peaks at around 2.3 and 2.0 V. The composite electrodes with 10 and 15 wt % copolymer exhibit much narrower reduction peaks compared to the composite electrode without copolymer or with low copolymer content. Narrow CV peaks imply that the active materials are confined in a highly ion/charge accessible environment. For the S-BP electrode without the copolymer, the anodic and cathodic peaks decrease after the first cycle. In contrast, for the electrodes with the copolymer, the cathodic peaks are rather stable during the five cycles, and only some decay in the anodic peaks is observed. The CV results indicate that the S-BP electrodes with the copolymer have better electrochemical stability than the S-BP electrode without copolymer due to the confined effect of the Pluronic copolymer. The composite electrode with 10 wt % copolymer was selected as a representative sample for comparing the cycling performance with the S-BP electrode without the copolymer.

Figure 5 shows the charge−discharge voltage profiles and cyclability of the S-BP electrodes with and without the Pluronic copolymer at 1*C* and 2*C* rates. Two discharge voltage plateaus at 2.3 and 2.0 V are observed for all the electrodes, which resemble the cathodic peaks in the CV. High initial discharge capacities of >1000 mA h g^{-1} were obtained for the electrodes as shown in Figure 5a. Although the electrodes with the copolymer show slightly lower initial capacities, they show higher capacities than the plain S-BP electrodes after 50 cycles (Figure 5b). The cycling performance in Figure 5c shows significant capacity drops during the first five cycles due to the dissolution of polysulfides into liquid electrolyte. Afterward, the electrodes with the Pluronic copolymer exhibit stable capacity retention during 50 cycles compared to the electrode without the copolymer. The improved cyclability of the composite electrodes with Pluronic copolymer indicates an electrochemically stable structure during cycling. The Coulombic efficiencies of these electrodes are above 97% after the initial 5 cycles, as shown in Figure 5d.

Figure 6a presents the cycle life of the composite electrodes with the Pluronic copolymer at 3*C* and 4*C* rates. The stabilized discharge capacities after 20 cycles are 520 and 470 mA h g^{-1}, respectively, at 3*C* and 4*C* rates with Coulombic efficiencies of >98%. The SEM images reveal that the cycled electrode without the copolymer (Figure 6b) contains agglomerated particles (white area) surrounded by carbon, whereas the cycled electrode with the copolymer (Figure 6c) is more uniform indicating the Pluronic copolymer could help maintain finely dispersed active material within the electrodes. Such a structure is beneficial for high rate cycling and capacity retention. To gain further understanding, we employed EIS to characterize the cells before and after 80 cycles, as shown in Figure 6d. There are two semicircles in these plots. The large semicircles at the high frequency region are related to the surface layers formed on the cathode and anode, the small semicircles at the medium-to-low frequency region are assigned to charge transfer resistance,[26,27] which are relatively constant for all cells before and after cycles. A slope at the low-frequency region corresponding to Warburg impedance is observed obviously for the cells containing the composite electrodes with Pluronic copolymer, which is attributed to lithium-ion diffusion limitations at the cathode and cathode/liquid interface[27] due to the copolymer surrounding the S-BP nanoparticles. This explains the low initial discharge capacities of the composite electrodes with the copolymer (Figure 5a). After 80 cycles, the resistance of the surface layer in the electrode without the copolymer is slightly decreased unlike the usual increase of those with conventional sulfur electrodes,[16] implying that the S-BP nanocomposite prevents the formation of a dense passivation layer (e.g., Li_2S) on the cathode.[28] The cell with the composite electrode containing the copolymer exhibits a significant reduction in the resistance of the surface layer due to the presence of Pluronic copolymer. The favorable performance obtained with the Pluronic copolymer in the S-BP composite electrodes demonstrates that it is a promising material for improving the electrochemical performance of Li−S batteries.

4. SUMMARY

A sulfur−carbon nanocomposite cathode material consisting of high-surface-area Black Pearls (BP) has been synthesized by an in situ deposition of sulfur on BP to give S-BP nanocomposites. The micropores of the carbon have been completely filled by sulfur and the surface of the carbon has been covered by sulfur, resulting in a significant reduction of the BET surface area of BP. The S-BP composite cathode shows high initial discharge capacity. The replacement of the conventional PVdF binder by the Pluronic block copolymer during electrode fabrication leads to the formation of a confined structure surrounding the S-BP nanoparticles, resulting in significant improvement in the capacity retention at high rates. The Pluronic copolymer also helps maintain a uniform electrode structure and reduce the impedance during cycling. The study demonstrates that the S-BP nanocomposite with a favorable nanostructure prepared through a solution process, combined with the use of Pluronic block copolymer during electrode fabrication, is promising for high-rate rechargeable Li−S batteries.

AUTHOR INFORMATION

Corresponding Author

*Tel: +1-512-471-1791. Fax: +1-512-471-7681. E-mail: manth@austin.utexas.edu.

Notes

The authors declare no competing financial interest.

ACKNOWLEDGMENTS

The authors thank Seven One Limited for the financial support.

REFERENCES

(1) Bruce, P. G.; Freunberger, S. A.; Hardwick, L. J.; Tarascon, J.-M. *Nat. Mater.* **2012**, *11*, 19−29.
(2) Herbert, D.; Ulam, J. U. S. Patent 3 043 896, 1962.
(3) Mikhaylik, Y. V.; Kovalev, I.; Schock, R.; Kumaresan, K.; Xu, J.; Affinito, J. *ECS Trans.* **2010**, *25*, 23−34.
(4) Ji, X.; Nazar, L. F. *J. Mater. Chem.* **2010**, *20*, 9821−9826.
(5) Mikhaylik, Y. V.; Akridge, J. R. *J. Electrochem. Soc.* **2004**, *151*, A1969−A1976.
(6) Akridge, J. R.; Mikhaylik, Y. V.; White, N. *Solid State Ionics* **2004**, *175*, 243−245.
(7) Ji, X.; Lee, K. T.; Nazar, L. F. *Nat. Mater.* **2009**, *8*, 500−506.
(8) Liang, C.; Dudney, N. J.; Howe, J. Y. *Chem. Mater.* **2009**, *21*, 4724−4730.

(9) Zhang, B.; Qin, X.; Li, G. R.; Gao, X. P. *Energy Environ. Sci.* **2010**, *3*, 1531−1537.
(10) Jayaprakash, N.; Shen, J.; Moganty, S. S.; Corona, A.; Archer, L. A. *Angew. Chem., Int. Ed.* **2011**, *50*, 5904−5908.
(11) Guo, J.; Xu, Y.; Wang, C. *Nano Lett.* **2011**, *11*, 4288−4294.
(12) Schuster, J.; He, G.; Mandlmeier, B.; Yim, T.; Lee, K. T.; Bein, T.; Nazar, L. F. *Angew. Chem., Int. Ed.* **2012**, *51*, 3591−3595.
(13) Evers, S.; Nazar, L. F. *Chem. Commun.* **2012**, *48*, 1233−1235.
(14) Yang, Y.; Yu, G.; Cha, J. J.; Wu, H.; Vosgueritchian, M.; Yao, Y.; Bao, Z.; Cui, Y. *ACS Nano* **2011**, *5*, 9187−9193.
(15) Wang, H.; Yang, Y.; Liang, Y.; Robinson, J. T.; Li, Y.; Jackson, A.; Cui, Y.; Dai, H. *Nano Lett.* **2011**, *11*, 2644−2647.
(16) Su, Y.-S.; Manthiram, A. *Electrochim. Acta* **2012**, *77*, 272−278.
(17) Park, G.-G.; Sohn, Y.-J.; Yim, S.-D.; Yang, T.-H.; Yoon, Y.-G.; Lee, W.-Y.; Eguchi, K.; Kim, C.-S. *J. Power Sources* **2006**, *163*, 113−118.
(18) Wang, G.; Sun, G.; Wang, Q.; Wang, S.; Sun, H.; Xin, Q. *Int. J. Hydrogen Energy* **2010**, *35*, 11245−11253.
(19) Sun, W.; Hsu, A.; Chen, R. *J. Power Sources* **2011**, *196*, 627−635.
(20) Pognon, G.; Brousse, T.; Belanger, D. *Carbon* **2011**, *49*, 1340−1348.
(21) Rettig, S. J.; Trotter, J. *Acta Crystallogr., Sect. C* **1987**, *43*, 2260−2262.
(22) Sakai, T.; Alexandridis, P. *Langmuir* **2004**, *20*, 8426−8430.
(23) Kabanov, A. V.; Alakhov, V. Y. *Crit. Rev. Ther. Drug Carrier Syst.* **2002**, *19*, 1−72.
(24) Abdullin, T. I.; Bondar, O. V.; Shtyrlin, Y. G.; Kahraman, M.; Culha, M. *Langmuir* **2010**, *26*, 5153−5159.
(25) Bruce, P. G.; Vincent, C. A. *J. Chem. Soc. Faraday Trans.* **1993**, *89*, 3187−3203.
(26) Fu, Y.-Z.; Manthiram, A. *J. Phys. Chem. C* **2012**, *116*, 8910−8915.
(27) Kolosnitsyn, V. S.; Kuz'mina, E. V.; Karaseva, E. V.; Mochalov, S. E. *Russ. J. Electrochem.* **2011**, *47*, 793−798.
(28) Cheon, S.-E.; Ko, K.-S.; Cho, J.-H.; Kim, S.-W.; Chin, E.-Y.; Kim, H.-T. *J. Electrochem. Soc.* **2003**, *150*, A800−A805.